Astrocyte Inositol Triphosphate Receptor Type 2 and Cytosolic Phospholipase A₂ Alpha Regulate Arteriole Responses in Mouse Neocortical Brain Slices

Lihua He[1], David J. Linden[2], Adam Sapirstein[1]*

1 Department of Anesthesiology and Critical Care Medicine, The Johns Hopkins University School of Medicine, Baltimore, Maryland, United States of America,
2 Department of Neuroscience, The Johns Hopkins University School of Medicine, Baltimore, Maryland, United States of America

Abstract

Functional hyperemia of the cerebral vascular system matches regional blood flow to the metabolic demands of the brain. One current model of neurovascular control holds that glutamate released by neurons activates group I metabotropic glutamate receptors (mGluRs) on astrocytes, resulting in the production of diffusible messengers that act to regulate smooth muscle cells surrounding cerebral arterioles. The acute mouse brain slice is an experimental system in which changes in arteriole diameter can precisely measured with light microscopy. Stimulation of the brain slice triggers specific cellular responses that can be correlated to changes in arteriole diameter. Here we used inositol trisphosphate receptor type 2 (IP_3R2) and cytosolic phospholipase A_2 alpha ($cPLA_2\alpha$) deficient mice to determine if astrocyte mGluR activation coupled to IP_3R2-mediated Ca^{2+} release and subsequent $cPLA_2\alpha$ activation is required for arteriole regulation. We measured changes in astrocyte cytosolic free Ca^{2+} and arteriole diameters in response to mGluR agonist or electrical field stimulation in acute neocortical mouse brain slices maintained in 95% or 20% O_2. Astrocyte Ca^{2+} and arteriole responses to mGluR activation were absent in $IP_3R2^{-/-}$ slices. Astrocyte Ca^{2+} responses to mGluR activation were unchanged by deletion of $cPLA_2\alpha$ but arteriole responses to either mGluR agonist or electrical stimulation were ablated. The valence of changes in arteriole diameter (dilation/constriction) was dependent upon both stimulus and O_2 concentration. Neuron-derived NO and activation of the group I mGluRs are required for responses to electrical stimulation. These findings indicate that an mGluR/IP_3R2/$cPLA_2\alpha$ signaling cascade in astrocytes is required to transduce neuronal glutamate release into arteriole responses.

Introduction

Blood flow to the brain is precisely regulated to match regional perfusion with metabolic requirements. Local activation of neurons produces signals that increase regional cerebral blood flow (rCBF) in a process known as functional hyperemia. Conversely, increases in arterial perfusion pressure are countered by pressure-induced increases in myogenic tone to stabilize blood flow. Thus the cerebral vasculature is able to maintain appropriate rCBF by both vasodilation and vasoconstriction.

Recent experimental work has established a model of cerebral vascular regulation that has at its center an astrocyte-dependent signaling pathway (reviewed [1,2]). The cytoarchitecture of astrocytes makes such a model feasible because they form a physical bridge between neural synapses and vascular structures. Astrocyte processes envelop many glutamatergic synapses and these same astrocytes also send specialized foot processes that cover the blood vessels of the brain [3,4]. In one current model of neurovascular regulation, activation of excitatory neurons results in the presynaptic release of glutamate (and sometimes other neurotransmitters). Glutamate interacts with neuronal post-synaptic receptors but can also bind group I mGluRs of a nearby

astrocyte. Early work supporting this model found that vascular responses were prevented by antagonists of group I metabotropic glutamate receptors (mGluR) and were triggered by agonist-induced activation of the mGluR [5].

Astrocyte mGluR activation is coupled to Gq and activates phospholipase C which hydrolyzes phosphatidylinositol 4,5-bisphosphate from cellular membranes to produce inositol 1,4,5-trisphosphate (IP_3) and 1,2-diacylglycerol (DAG). IP_3 then binds a cognate receptor, the IP_3R, on the cytosolic face of the endoplasmic reticulum. Within astrocytes of the neocortex the only form of IP_3R expressed is the type 2 IP_3R (IP_3R2). IP_3R2 binding opens a Ca^{2+} channel within the receptor causing Ca^{2+} mobilization from internal stores [6]. Consistent with this portion of the model, direct mechanical activation of astrocytes in cortical brain slices caused arteriolar dilation which was eliminated by the cell-permeant Ca^{2+} chelator BAPTA/AM [5].

The phospholipases A_2 (PLA_2s) are a family of enzymes that hydrolyze a free fatty acid from the sn-2 position of membrane glycerolphospholipids and are highly expressed in the brain [7]. Previous experiments have suggested that increases in astrocyte Ca^{2+} can activate Ca^{2+}-dependent PLA_2 and that a Ca^{2+}-dependent PLA_2 is needed for cerebrovascular regulation [8].
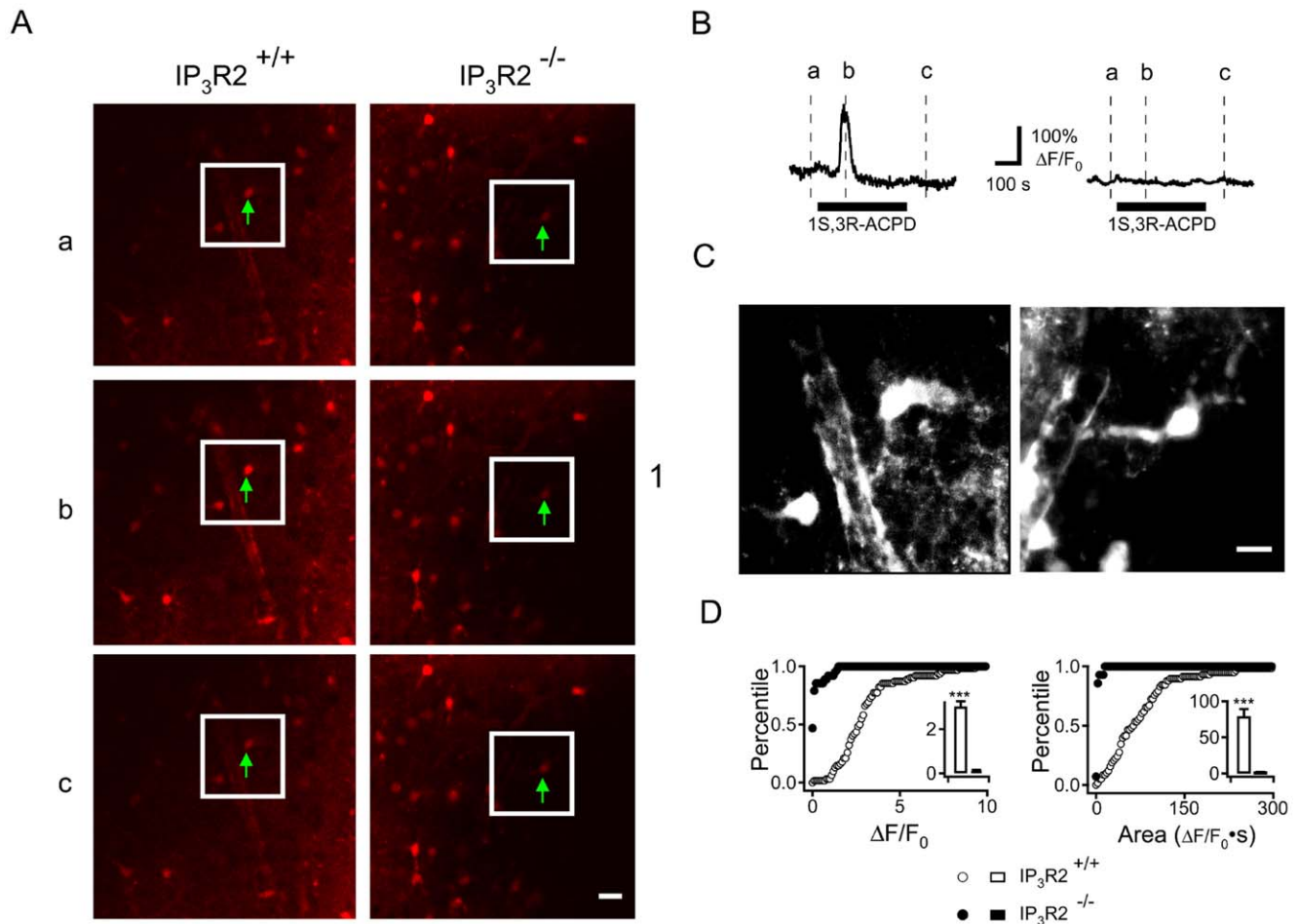
Figure 1. Astrocyte Ca^{2+} responses to mGluR agonist application are attenuated IP$_3$R2$^{-/-}$ slices. A. Neocortical brain slices from IP$_3$R2$^{+/+}$ (left panel) and IP$_3$R2$^{-/-}$ (right panel) mice were loaded with the Ca^{2+}-sensitive fluorophore Rhod-2/AM and astrocytes were identified by dye uptake, morphology and location. Ca^{2+} fluorescence was measured in the region of interest (green arrow) and is displayed at 3 time points in relation to 1S,3R-ACPD treatment: (a) before, (b) at peak response and (c) after. White outline indicates the region of magnification in C. Scale bar: 20 μm. **B.** Fluorescence intensity signals for the Ca^{2+} fluorescence measured in the soma of the indicated astrocytes. Signals were corrected for background that was measured in an identical area immediately adjacent to the region of interest. Representative single traces of the Ca^{2+} response in soma of IP$_3$R2$^{+/+}$ astrocytes (left trace) and IP$_3$R2$^{-/-}$ (right trace) are shown and the duration of 1S, 3R-ACPD application is indicated below the traces. **C.** Z-stack of 12 images encompassing 12 mm of depth in IP$_3$R2$^{+/+}$ (left panel) and IP$_3$R2$^{-/-}$ (right panel) brain slices. This demonstrates the ameboid shape of the astrocyte soma which extends a foot process near a neighboring arteriole. Scale Bar: 10 μm. **D.** Cumulative probability histograms of population responses are shown. Peak (left panel) and integrated (right panel) Ca^{2+} responses of IP$_3$R2$^{+/+}$ (open circles, 58 cells) and IP$_3$R2$^{-/-}$ (filled circles, 63 cells) astrocytes with inset bar graphs indicating the mean ± S.E.M. Nine slices were prepared from four mice for each genotype. doi:10.1371/journal.pone.0042194.g001

Thus, the next step in the model is that PLA$_2$ releases arachidonic acid which is metabolized by cyclooxygenase enzymes to form prostaglandin (PG) H$_2$ and by epoxygenase enzymes to form epoxyeicosatrienoic acids (EETs). PGH$_2$ is rapidly metabolized by terminal synthase enzymes to any of the PGs. The PGs have demonstrated vascular effects that are mediated through prostaglandin and thromboxane receptors located on the extracellular surface of vascular smooth muscle cells (VSMC). It appears that cerebral metabolism is coupled to PGE$_2$-dependent vasoregulation. A low oxygen tension in brain slices increases glycolysis which produces lactate which reduces PGE$_2$ uptake by astrocyte prostaglandin transporters [9]. Increased extracellular PGE$_2$ dilates cerebral arterioles while cyclooxygenase inhibitors prevent vasomotor response [9,10].

While there is some experimental evidence to support this model of neurovascular regulation, many details remain unresolved. For example, experiments supporting the present model

have relied on photolysis of caged IP$_3$ in astrocytes to trigger vascular responses [11]. However photo-activation of caged IP$_3$ releases supraphysiologic levels of IP$_3$ and does so in a way that may not represent the spatially-regulated release from subcellular compartments. In addition, the roles of PLA$_2$s in neurovascular regulation have been principally examined by using pharmacologic inhibitors that are not specific for single PLA$_2$ isoforms and do not target specific cell types. Mammalian brain tissue expresses, and has enzymatic activity for all of, the major PLA$_2$s including Ca^{2+}-independent (iPLA2, GVIA), Ca^{2+}-dependent secretory PLA$_2$s (groups IIA, V and X) and the cytosolic PLA$_2$s (cPLA$_2$, GIV) [7]. The group IVA PLA$_2$ (cytosolic PLA$_2$α, cPLA$_2$α) is of particular interest because its translocation to specific cellular membranes is highly regulated and its enzymatic activity is enhanced by phospholipids that have arachidonate at the sn-2 position [12]. These pharmacologic inhibitors have effects on

different forms of PLA$_2$ and may also have side-effects that are unrelated to PLA$_2$ blockade [13,14].

Here we have sought to determine the molecular constituents of astrocyte Ca^{2+} signaling and PLA$_2$ activation in the cerebrovascular regulatory pathway. To do this we compared responses of cortical astrocytes and their neighboring arterioles in cortical brain slices derived from mice that were deficient in IP$_3$R2 or cPLA$_2\alpha$.

Results

In one current model of neurovascular regulation it is postulated that activation of astrocyte mGluR by glutamate leads to activation of PLC which releases IP$_3$. The free IP$_3$ binds to IP$_3$ receptors on the endoplasmic reticulum thus opening Ca^{2+} channels and increasing intracellular Ca^{2+} [8]. There are three IP$_3$R isoforms but the type 2 receptor (IP$_3$R2) appears to be the only form expressed in glial cells within the CNS [15,16]. Therefore we measured the astrocyte Ca^{2+} and arteriole responses to stimulation of cortical brain slices from mice deficient in the type 2 IP$_3$R (IP$_3$R2$^{-/-}$) and their wild-type littermates (IP$_3$R2$^{+/+}$).

We incubated acute cortical slices from IP$_3$R2$^{+/+}$ and IP$_3$R2$^{-/-}$ mice with a Ca^{2+} sensitive fluorophore, Rhod-2/AM, in a manner that preferentially loads astrocytes [8]. After washout of unloaded dye and a period of equilibration in artificial CSF (ACSF) we introduced the metabotropic glutamate receptor agonist, 1S,3R-ACPD (50 µM) to the bath and examined the Ca^{2+} responses with confocal fluorescence microscopy (Figure 1A). Signals were measured in the soma of cortical astrocytes. These astrocytes were identified by their location, somatic morphology and the presence of a foot process extending from the soma (Figure 1C). In the IP$_3$R2$^{+/+}$ slices there were robust increases in the Ca^{2+} signals in cells that were morphologically identified as astrocytes, while in the IP$_3$R2$^{-/-}$ slices such Ca^{2+} responses were absent (Figure 1B and D) (IP$_3$R2$^{+/+}$, $\Delta F/F_0 = 302.4 \pm 23.5\%$, Time Integrated F/F$_0$ = 78.8. ±10.3. IP$_3$R2$^{-/-}$, no detectable Ca^{2+} signal. $P < 0.001$. n = 58 IP$_3$R2$^{+/+}$ and 63 IP$_3$R2$^{-/-}$ cells from 4 mice for each genotype).

We measured changes in the diameter of arterioles in cortical brain slices from IP$_3$R2$^{+/+}$ and IP$_3$R2$^{-/-}$ mice in response to 1S,3R-ACPD (Figure 2). Populations of arterioles were selected as described in Methods so that the mean diameters before any treatment were similar in the IP$_3$R2$^{+/+}$ and IP$_3$R2$^{-/-}$ slices. After equilibration in ACSF with 95% O$_2$ and 5% CO$_2$ the diameters of IP$_3$R2$^{+/+}$ (n = 18) and IP$_3$R2$^{-/-}$ arterioles (n = 24) were 11.8±1.1 µm and 10.1±0.8 µm respectively ($P = 0.20$). In the 95% O$_2$ environment, treatment of IP$_3$R2$^{+/+}$ slices with 1S,3R-ACPD caused significant arteriole constriction while the IP$_3$R2$^{-/-}$ arterioles did not respond (Figure 2A, B) (IP$_3$R2$^{+/+}$, 8.8±1.7%, $vs.$ IP$_3$R2$^{-/-}$, 0.8±1.5%; $P < 0.01$). Prostaglandin E$_2$ (PGE$_2$) is a vasoactive metabolite of arachidonic acid that is thought to participate in vascular regulation through activation of prostaglandin E receptors (reviewed in [17]). Arterioles in IP$_3$R2$^{+/+}$ and IP$_3$R2$^{-/-}$ mice had the same constrictive response to treatment with PGE$_2$ (IP$_3$R2$^{+/+}$, −35.7±4.3% $vs.$ IP$_3$R2$^{-/-}$, −34.1±2.6%; $P = 0.74$) which indicates the mechanisms for prostaglandin-dependent vasoregulation are downstream from astrocyte IP$_3$ signaling and that arterioles in IP$_3$R2$^{-/-}$ mice are not generally deficient in constrictive function. Other investigators have suggested that the pre-existing level of vascular tone (diameter) determines the vasomotor response to mGluR activation [10] and have postulated that vessels without myogenic tone, as is the case in brain slices, do not represent a physiologic state [2]. In order to simulate physiologic levels of arteriolar tone we bath-applied U-46619, a stable analog of PGH$_2$, that is a selective thromboxane receptor agonist [18]. U-46619 (1 µM) caused complete occlusion of many arterioles while

lower doses resulted in continuous arteriole constriction with a slope that was dose-dependent (not shown). We applied 100 nM U-46619 because it constricted the arterioles approximately 40% of the initial diameter within the equilibration period of the experiment (Supporting Figure S1). When cortical slices from IP$_3$R2$^{+/+}$ and IP$_3$R2$^{-/-}$ slices were pretreated with 100 nM U-46619 they constricted to the same degree (Constriction relative to diameter after 30 minutes of U-46619: IP$_3$R2$^{+/+}$, −78.9±10.6%, n = 16 vs. IP$_3$R2$^{-/-}$, −70.9±15.4%, n = 17; $P = 0.29$) (Figure 2C, inset). Supporting Figure S2 shows a representative trace of diameter from a single arteriole. Bath application of 1S,3R-ACPD (50 µM for 10 min) during U-46619 exposure caused significant IP$_3$R2+/+ arteriole dilation (16.1±3.5%, $P < .01$) while there was no response in the IP$_3$R2$^{-/-}$ arterioles (0.5±2.0%) when compared to IP$_3$R2+/ + slices that were not treated with 1S,3R-ACPD (n = 7) (Figure 2C).

Treatment with 1S,3R-ACPD initiates the vasoregulatory pathway at the point of astrocyte mGluR activation and thus bypasses upstream signaling in neurons. In order to examine the role of the astrocyte IP$_3$ signaling on neurovascular coupling following activation of neurons we performed electrical field stimulation in the cortical brain slices. We stimulated a cortical field with a bipolar electrode using 100 Hz for 200 ms repeated 48 times over a 4 min period and examined the arteriolar responses 200–300 µm from the electrode. We determined that this 100 Hz stimulation increased astrocyte somatic intracellular Ca^{2+} consistent with their robust activation (Supporting Figure S3). In contrast to treatment with 1S,3R-ACPD, electrical field stimulation caused significant dilation in IP$_3$R2$^{+/+}$ arterioles, which peaked 15 min after stimulation (5.45±1.7%, n = 15). There was an insignificant constriction of 1.70±0.92% in the IP$_3$R2$^{-/-}$ slices (Figure 3A) (n = 14; $P < 0.01$ compared to IP$_3$R2$^{+/+}$ between 5–30 minutes following stimulation). When the slices were pre-treated with U-46619 (50 nM), electrical stimulation caused a significant dilatory response in the IP$_3$R2$^{+/+}$ arterioles when compared to the continuous constriction observed in the IP$_3$R2$^{-/-}$ slices (Figure 3B) (IP$_3$R2$^{+/+}$, −2.8±3.1% vs. IP$_3$R2$^{-/-}$, −22.2±5.0%; measured 15 minutes after electrical stimulation, expressed relative to diameter at start of stimulation; $P < 0.01$).

In contrast to our results, a previous study in rat hippocampal slices found that electrical stimulation in a high O$_2$ environment caused arteriole constriction [9]. However, in a low O$_2$ environment, electrical stimulation caused arteriole dilation [9]. Therefore we wished to determine if O$_2$ tension alters the response to electrical stimulation of murine cortical slices. When electrical stimulation was delivered to IP$_3$R2$^{+/+}$ and IP$_3$R2$^{-/-}$ slices equilibrated in 20% O$_2$ the responses were identical to those observed in 95% O$_2$ (Figure 3C, compare to 3A). To determine if electrical stimulation of neurons causes dilation by activation of the astrocyte mGluR, slices from IP$_3$R2$^{+/+}$ were treated with the mGlu$_5$ antagonist, 2-Methyl-6-(phenylethynyl)pyridine hydrochloride (MPEP) (10 µM) and the mGlu$_1$ antagonist JNJ 16259685 (100 nM) before electrical stimulation. Blockade of these group I mGluRs prevented the arteriole dilation response to stimulation (Figure 3C). Taken together these results show that, glutamatergic activation of astrocyte mGluRs results in IP$_3$R2 receptor-mediated increases in astrocyte Ca^{2+} that are necessary for either constriction or dilation of arterioles. The direction of the change in arteriole diameter depends on the pre-existing state of the vessel (U-46619 pre-treatment) and also the mode of activation (1S, 3R-ACPD vs. electrical stimulation).

Increases in astrocyte Ca^{2+} are postulated to activate one or more forms of Ca^{2+}-dependent PLA$_2$ and PLA$_2$ activity may be the rate limiting step in the generation of vasoactive eicosanoids [19]. Because of the unique biochemical and molecular properties
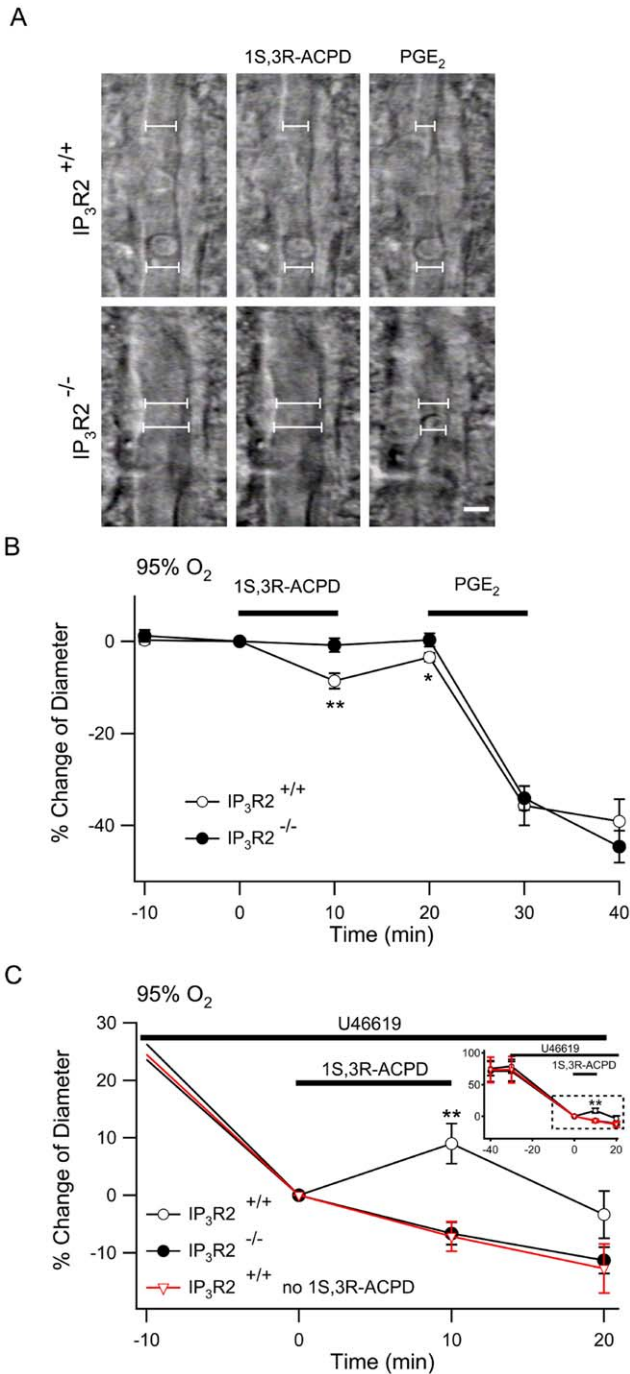
Figure 2. Arteriole responses to mGluR agonist application are eliminated in IP$_3$R2$^{-/-}$ neocortical slices. A. Gradient contrast imaging was used to measure arteriole responses to treatment. Responses to 1S,3R-ACPD were quantified by defining 6 points (2 of the points are shown in this figure) at which to measure changes in arteriole diameter over time (described in Methods). The arteriole diameter is expressed as the average diameter of the points. Scale bar: 5 μm. **B.** Cortical slices from IP$_3$R2$^{+/+}$ (open circle, n = 18) and IP$_3$R2$^{-/-}$ (filled circle, n = 24) were treated with 1S,3R-ACPD followed by PGE$_2$ and arteriole responses were measured. **C.** During continuous application of U-46619 the IP$_3$R2$^{+/+}$ and IP$_3$R2$^{-/-}$ were treated with 1S,3R-ACPD while another group of IP$_3$R2$^{+/+}$ slices were treated with vehicle instead of 1S,3R-ACPD (red inverted triangle, n = 7). Inset shows the complete experiment from the time of application of U-46619. The dashed white box indicates the expanded graph. Treatment with U-46619 (100 nM) constricted arterioles of both IP$_3$R2$^{+/+}$ (n = 16) and IP$_3$R2$^{-/-}$ slices

(n = 17) to a similar extent. **, $P < 0.01$ comparing IP$_3$R2$^{+/+}$ to IP$_3$R2$^{-/-}$ 10 min following 1S, 3R-ACPD application.
doi:10.1371/journal.pone.0042194.g002

of cPLA$_2\alpha$ we explored arteriole responses in acute cortical brain slices derived from cPLA$_2\alpha^{+/+}$ and cPLA$_2\alpha^{-/-}$ mice. Once again we selected arterioles based on the histology and diameter of the vessel and determined that there was no difference in the arteriole diameters between cPLA$_2\alpha^{+/+}$ (11.6±1.3 μm, n = 29) and cPLA$_2\alpha^{-/-}$ neocortical slices (11.8±1.1 μm, n = 15). We repeated the 1S,3R-ACPD stimulation experiment in a 95% O$_2$ environment and found that in naïve cPLA$_2\alpha^{+/+}$ slices, arterioles constricted 12.2±1.9% in response to 1S,3R-ACPD. In contrast arterioles in slices of cPLA$_2\alpha^{-/-}$ neocortex did not constrict in response to 1S, 3R-ACPD (1.6±1.3%; $P < .001$ compared to cPLA$_2\alpha^{+/+}$, Figure 4A). We postulated that cPLA$_2\alpha$ serves to supply arachidonic acid and predicted that the response to exogenous PGE2 would be unaltered in cPLA$_2\alpha^{-/-}$ slices [5]. When 1S, 3R-ACPD was removed from the perfusate and replaced with 10 μM PGE2, arterioles of both the cPLA2α+/+ and cPLA$_2\alpha^{-/-}$ slices constricted identically (cPLA2α+/+, 35.1±5.2%; cPLA$_2\alpha^{-/-}$, 34.4±6.6%; Figure 4A).

To determine if cPLA$_2\alpha$-dependent responses were affected by the tension of the arteriole prior to activation we pre-treated slices with U-46619. Following 30 minutes of U-46619 exposure the degree of constriction in cPLA$_2\alpha^{+/+}$ (35.1±2.9%, n = 21) and cPLA$_2\alpha^{-/-}$ arterioles (31.6±2.4%, n = 25) was not different (Figure 4B). In the presence of U-46619, cPLA$_2\alpha^{+/+}$ arterioles continued to progressively constrict and were used as a control for drug treatment experiments (n = 10). We applied 1S,3R-ACPD 50 μM which caused a significant 13.9±2.2% dilation in cPLA$_2\alpha^{+/+}$ arterioles when compared to slices that were treated with vehicle instead of 1S,3R-ACPD (n = 10) (Figure 4B; normalized to U-46619 preconstricted arteriole diameters immediately before treatment with 1S,3R-ACPD or vehicle; $P < .01$, 15 min following electrical stimulation). In contrast, the arterioles of cPLA$_2\alpha^{-/-}$ slices did not respond to 1S,3R-ACPD treatment (0.9±1.8%). To ensure that the results measured in the cPLA$_2\alpha^{-/-}$ slices were due to loss of enzymatic activity and not an unrelated mechanism compensating for gene deletion, we pretreated cPLA$_2\alpha^{+/+}$ slices with 10 μM ATK (n = 21), a mixed iPLA$_2$/cPLA$_2\alpha$ inhibitor, during the 30 min U-46619 preconstriction. ATK treatment prevented dilation in the 1S,3R-ACPD-treated cPLA$_2\alpha^{+/+}$ arterioles and resulted in a small constrictive response to 1S,3R-ACPD when compared to slices that were treated with U-46619 but not 1S,3R-ACPD (ATK/U-46619/ 1S,3R-ACPD-treated −15.2±2.1%, compared to U-46619-treated −7.9±3.3%; $P < 0.05$).

In a previous investigation the polarity of arteriole response to t-ACPD was dependent upon oxygen content of the slice media [9]. A low oxygen environment appeared to enhance glycolysis with increased lactate and PGE$_2$ levels and resulted in dilation of arterioles [9]. Therefore we equilibrated slices from cPLA$_2\alpha^{+/+}$ and cPLA$_2\alpha^{-/-}$ mice in 20% O$_2$ and 5% CO$_2$ before and during treatment with 1S, 3R-ACPD. In low O$_2$, pharmacological activation of the mGluR resulted in dilation of the cPLA$_2\alpha^{+/+}$ arterioles while cPLA$_2\alpha^{-/-}$ arterioles remained unresponsive (Figure 4C). Interestingly the 20% O$_2$ environment also reversed the polarity of the response to 10 μM PGE$_2$, causing arteriole dilation in both genotypes (Figure 4C). Taken together these results show that cPLA$_2\alpha$ is required for the vascular responses to 1S,3R-ACPD stimulation of the mGluR. Importantly, cPLA$_2\alpha$ reaction products and their metabolites can trigger either arteriole constriction or dilation, depending on the initial condition and the metabolic state of the vessel.
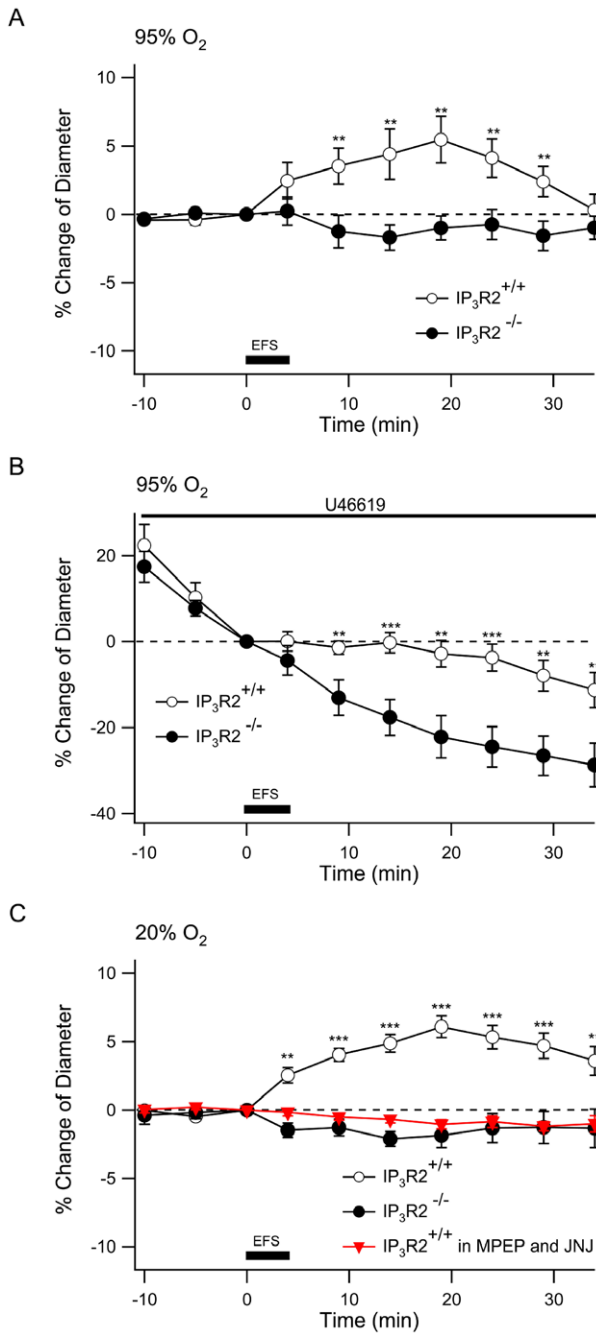
Figure 3. Neocortical arterioles of IP$_3$R2$^{-/-}$ slices do not respond to electrical field stimulation. A. Responses of arterioles in 95% O$_2$ following electrical field stimulation. Cortical slices from IP$_3$R2$^{+/+}$ (open circle) and IP$_3$R2$^{-/-}$ mice (closed circle) were treated with electrical field stimulation (EFS) of 100 Hz trains of 200 ms at 0.2 Hz for 4 minutes as indicated by the dark bar. Arteriole diameter was measured every 5 min during the experiment. IP$_3$R2$^{+/+}$, n = 15; IP$_3$R2$^{-/-}$ n = 15. ****,** $P < 0.01$, IP$_3$R2$^{+/+}$ compared to IP$_3$R2$^{-/-}$. **B.** Pretreatment with U-46619 for 30 min was followed by electrical stimulation and arteriole diameters of IP$_3$R2$^{-/-}$ were compared to IP$_3$R2$^{+/+}$. IP$_3$R2$^{+/+}$, n = 15; IP$_3$R2$^{-/-}$ n = 14. ****,** $P < 0.01$; *****,** $P < 0.001$. **C.** Blockade of Group I mGluR with MPEP and JNJ prevents arteriole responses to electrical stimulation in IP$_3$R2$^{+/+}$ slices (inverted triangles) while a 20% O2 environment does not alter responses of naïve IP$_3$R2$^{+/+}$ or IP$_3$R2$^{-/-}$ arterioles. IP$_3$R2$^{+/+}$, n = 14; IP$_3$R2$^{-/-}$ n = 12, IP$_3$R2$^{+/+}$ with MPEP/JNJ, n = 9. ****,** $P < 0.01$; *****,** $P < 0.001$.
doi:10.1371/journal.pone.0042194.g003
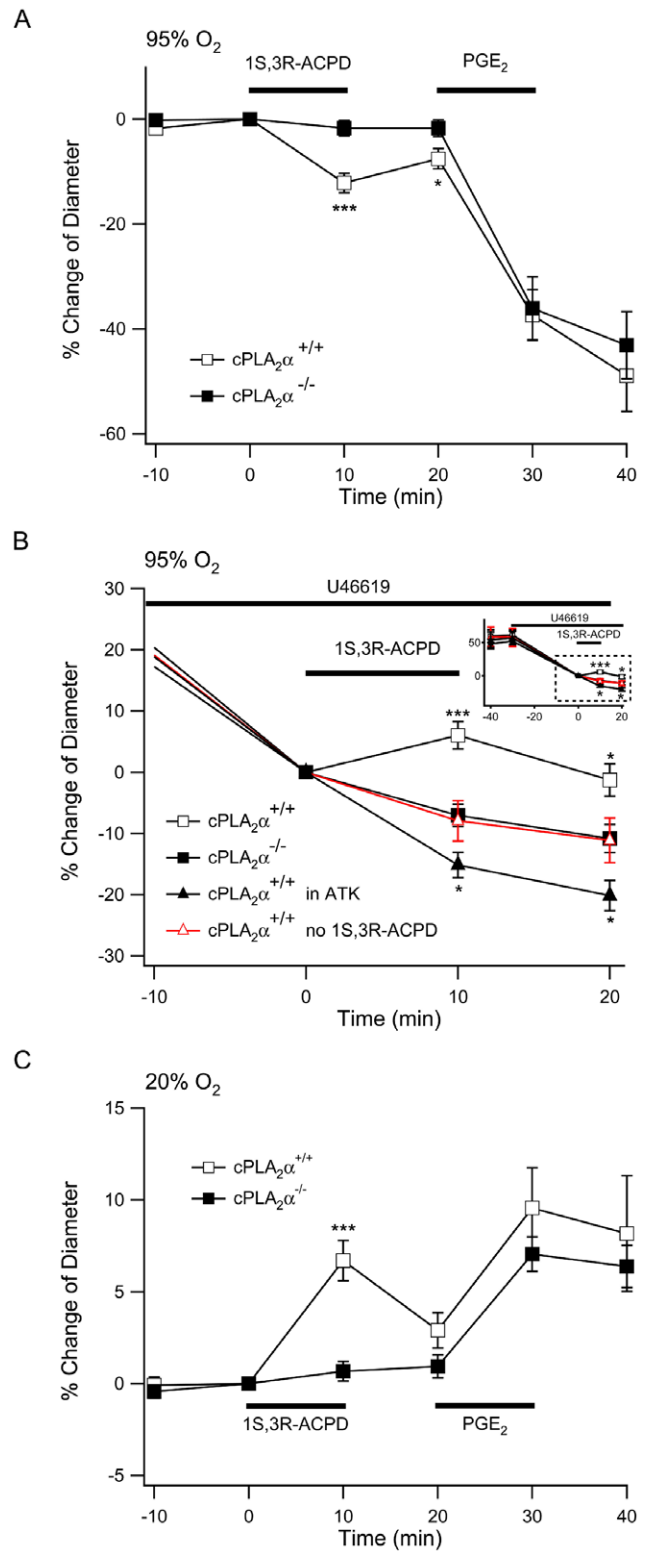
Figure 4. Arteriole responses to mGluR agonist application are eliminated in cPLA$_2\alpha^{-/-}$ neocortical slices. A. Bath application of 1S,3R-ACPD 50 μM to slices equilibrated with 95% O$_2$ induced constriction of arterioles in cortical slices of cPLA$_2\alpha^{+/+}$ (empty square, n = 29), but not cPLA$_2\alpha^{-/-}$ mice (filled square, n = 15). Washout of 1S,3R-ACPD was followed by application of 10 μM PGE$_2$ which caused identical constriction of arterioles in both genotypes. **B.** In slices at equilibrium with 95% O$_2$, arterioles were preconstricted with 100 nM U-

46619 supplemented ACSF. To compare acute cPLA$_2\alpha$ inhibition with gene deletion, cPLA$_2\alpha^{+/+}$ slices were treated with 10 μM ATK (filled black triangle, n = 21) for the duration of the experiment. Inset shows the complete experiment from the time of application of U-46619. The dashed white box indicates the expanded graph. After 30 min equilibration in U-46619, 1S,3R-ACPD was added to the bath at a final concentration of 50 μM (time = 0) and the responses of arterioles in cPLA$_2\alpha^{+/+}$ (n = 21) and cPLA$_2\alpha^{-/-}$ (n = 25) cortical slices were compared to cPLA$_2\alpha^{+/+}$ slices that were not treated with 1S,3R-ACPD (red empty triangle, n = 10). *, P<0.05; **, P<0.01; ***, P<0.001. **C.** When slices were equilibrated in 20% O$_2$, 1S,3R-ACPD treatment dilated cPLA$_2\alpha^{+/+}$ (n = 18) but not cPLA$_2\alpha^{-/-}$ (n = 16) arterioles. Bath application of 10 μM PGE$_2$ caused dilation of both genotypes. ***, P<0.001.
doi:10.1371/journal.pone.0042194.g004

If increased astrocyte Ca^{2+} is directly coupled to activation of cPLA$_2\alpha$ then we predicted that cPLA$_2\alpha$ would be necessary for the arteriole response to electrical stimulation in cortical brain slices. We subjected cortical slices, in 95% O$_2$, from cPLA$_2\alpha$+/+ and cPLA$_2\alpha^{-/-}$ mice to the same electrical stimulation protocol used previously. The cPLA$_2\alpha$+/+ arterioles had a small but significant dilation while the cPLA$_2\alpha^{-/-}$ arterioles constricted slightly in response to the electrical stimulation (Figure 5A) (20 min after stimulation, cPLA$_2\alpha$+/+, 6.1±2.5%, n = 23 compared to cPLA$_2\alpha^{-/-}$, −2.8±1.1%, n = 23, P<0.01). To determine if the vascular tone of the arteriole impacts the response to electrical stimulation we applied a lower dose of U-46619, 20 nM, to the slice perfusate. This treatment caused arteriole constriction that was the same in cPLA$_2\alpha$+/+ and cPLA$_2\alpha^{-/-}$ slices (Figure 5B). When electrical stimulation was applied to U-46619-treated cPLA$_2\alpha$+/+ slices there was a highly significant dilation response when compared to arterioles that were treated with U-46619 but not electrically stimulated (Figure 5B). This response became significant 10 min following electrical stimulation and continued through the 30 minute measurement period. In contrast there was no response of the cPLA$_2\alpha^{-/-}$ arterioles to electrical stimulation when compared to unstimulated slices (Figure 5B) (20 minutes after stimulation, cPLA$_2\alpha$+/+, −2.6±4.3%, n = 23; cPLA$_2\alpha^{-/-}$, −30.3±4.3%, n = 23; and cPLA$_2\alpha$+/+, without electrical stimulation, −21.5±3.5%, n = 9; all diameters relative to the diameter at time of the onset of electrical stimulation. P<0.01 for cPLA$_2\alpha^{+/+}$ compared to cPLA$_2\alpha^{+/+}$ without simulation). The results thus far show that 1S,3R-ACPD (isolated mGluR activation) causes constriction in naïve cPLA$_2\alpha$+/+ slices while electrical stimulation (which includes neuron activation) causes dilation. Neurons must therefore modulate vascular responses by trans-cellular activation of the astrocyte mGluR and a second mGluR-independent mechanism. This mGluR-independent mechanism must also be cPLA$_2\alpha$-dependent since arterioles in cPLA$_2\alpha^{-/-}$ slices also failed to respond to electrical stimulation.

We wished to understand the role of cPLA$_2\alpha$ in arteriole regulation following electrical stimulation. Neuronal nitric oxide synthase (nNOS) is thought to be the only isoform that contributes to metabolic hyperemia [20]. In addition, neuronal nitric oxide (NO) has been postulated to modulate cerebrovascular responses by inhibition of arachidonic acid metabolism [21]. Therefore, we applied either 10 μM Nω-propyl-l-arginine (L-NPA), a specific nNOS antagonist, or vehicle to cPLA$_2\alpha^{+/+}$ slices equilibrated in 20% O$_2$. Slices that were treated with vehicle dilated in response to electrical stimulation just as they had in 95% O$_2$ (Figure 6). In contrast L-NPA-treated and cPLA$_2\alpha^{-/-}$ slices had a small constrictive response (Figure 6). Thus it appears that nNO plays a role in the generation of the cPLA$_2\alpha$-dependent production of a vasodilator compound.
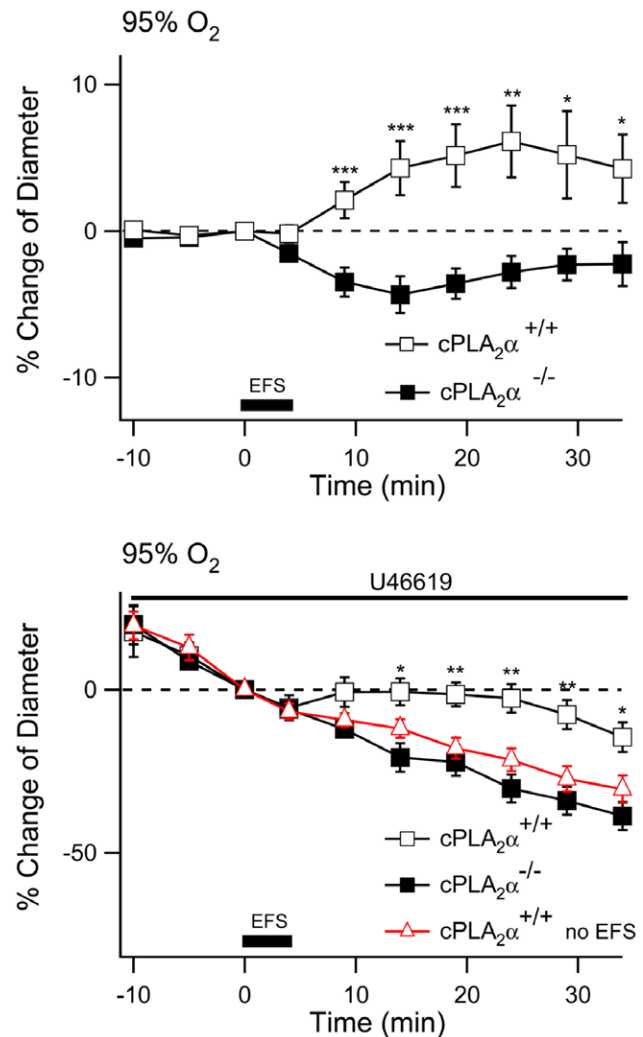
Figure 5. Arterioles of cPLA$_2\alpha^{-/-}$ neocortical slices do not dilate in response to electrical stimulation. A. Neocortical brain slices from cPLA$_2\alpha^{+/+}$ (empty square, n = 23) and cPLA$_2\alpha^{-/-}$ mice (filled square, n = 23) were stimulated with 100 Hz trains of 200 ms at 0.2 Hz for 4 minutes as indicated by the dark bar (electrical field stimulation, EFS). Arteriole diameter was measured every 5 min during the experiment. *, P<0.05; **, P<0.01; *** P<0.001: cPLA$_2\alpha^{+/+}$ compared to cPLA$_2\alpha^{-/-}$. **B.** After treatment with 20 nM U-46619 for 30 min, electrical stimulation was applied to cortical slices from cPLA$_2\alpha^{+/+}$ and cPLA$_2\alpha^{-/-}$ mice and changes in arteriole diameter were compared to cPLA$_2\alpha^{+/+}$ arterioles that did not have electrical stimulation (red triangle, n = 9). *, P<0.05; **, P<0.01; *** P<0.001: cPLA$_2\alpha^{+/+}$ and cPLA$_2\alpha^{-/-}$ with electrical stimulation compared to cPLA$_2\alpha^{+/+}$ without electrical stimulation at the same time points.
doi:10.1371/journal.pone.0042194.g005

It is possible that cPLA$_2\alpha$ is necessary for normal Ca^{2+} responses to mGluR activation. In order to precisely determine if cPLA$_2\alpha$ alters the astrocyte Ca^{2+} response to 1S,3R-ACPD we crossed the cPLA$_2\alpha$ gene deficiency into a mouse line carrying a transgene that expresses the EGFP under the control of the S100β promoter [22]. These mice have a population of astrocytes that strongly express EGFP which can readily be identified by fluorescent microscopy. We prepared acute cortical slices from S100β-EGFP-cPLA$_2\alpha$+/+ and S100β-EGFP-cPLA$_2\alpha^{-/-}$ mice and loaded the slices with Rhod-2/AM. Using EGFP fluorescence we identified astrocytes and defined regions of interest (ROI) around the soma
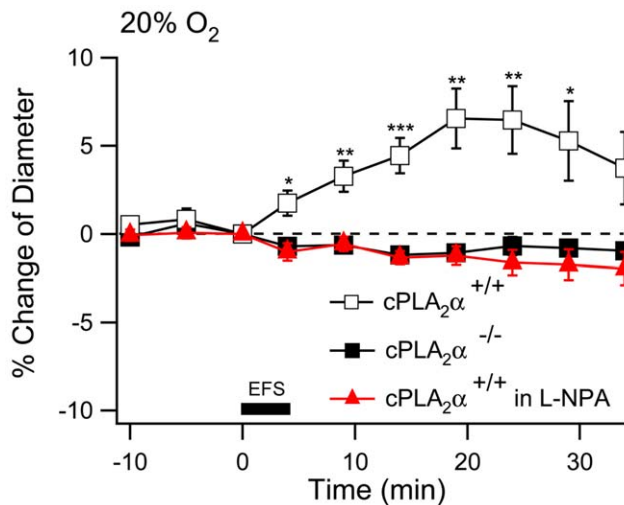
Figure 6. Inhibition of nNOS with L-NPA prevents dilation of arterioles following electrical stimulation. cPLA$_2\alpha^{+/+}$ slices were equilibrated in 20% O$_2$ and treated with ACSF (hollow square, n = 14;) or ACSF with 10 μM L-NPA 60 min before electrical stimulation (filled red triangle, n = 9). cPLA$_2\alpha^{-/-}$ (filled square, n = 9) were treated with ACSF. Electrical stimulation was applied as indicated by the dark bar (electrical field stimulation, EFS). *, $P < .05$; **, $P < .01$.
doi:10.1371/journal.pone.0042194.g006

and neighboring foot processes (Figure 7A). We measured the Ca^{2+} responses over time in the soma and foot processes of these cells following bath application of 1S,3R-ACPD 50 μM (Figure 7A). There were no differences between the cPLA$_2\alpha+/+$ and cPLA$_2\alpha^{-/-}$ genotypes in the Ca^{2+} responses as measured by amplitude, rise time, half width duration, decay time or total integrated signal in the soma (Figure 7B) (cPLA$_2\alpha+/+$, n = 169 cells; cPLA$_2\alpha^{-/-}$, n = 166 cells) or the foot processes (Figure 7C) (cPLA$_2\alpha+/+$, n = 36 endfeet; cPLA$_2\alpha^{-/-}$, n = 33 endfeet).

Discussion

We have used mutant mice to identify IP$_3$R2 and cPLA$_2\alpha$ as essential elements for the transduction of neuronal activity into vascular responses in an acute neocortical brain slice model. We found that IP$_3$R2 and cPLA$_2\alpha$ are necessary for both constrictive and dilatory responses following activation of the astrocyte mGluR by 1S,3R-ACPD. Furthermore electrical stimulation of brain slices caused arteriole dilation which was dependent on IP$_3$R2, cPLA$_2\alpha$ and neuron-derived NO. The increase in astrocyte intracellular Ca^{2+} following application of 1S,3R-ACPD requires IP$_3$R2 but not cPLA$_2\alpha$. These results are the first demonstration that the effector of mGluR-evoked Ca^{2+} response in astrocytes is the IP3R2 and that this receptor and cPLA$_2\alpha$ are essential for cortical cerebrovascular regulation.

Many of the biochemical steps involved in the neuron-to-astrocyte-to-vascular smooth muscle cell signal transduction process have been defined. The sufficiency of astrocyte Ca^{2+} transients to initiate arteriole responses in brain slices was demonstrated by photo-uncaging of Ca^{2+} within astrocytes [8] and photolysis of caged IP$_3$ in retinal Mueller cells which triggered both a Ca^{2+} response in the Mueller cell and vasodilation [11]. Thus, previous work is supportive of the model but photolysis may have had effects on cells other than the targeted astrocytes. Previously, use of IP$_3$R2 knockout mice demonstrated that IP$_3$R2 is required for the Ca^{2+} responses of hippocampal astrocytes to a combination of chemical G-protein coupled receptor activators

[15]. Because IP$_3$R2 is the only IP$_3$R isoform that is expressed in astrocytes [15], we reasoned that if astrocyte IP$_3$ is an essential effector of vascular responses to astrocyte mGluR activation then the signal must be transduced through the IP$_3$R2. This reasoning is supported by the finding that IP$_3$R2$^{-/-}$ cortical slices failed to respond to mGluR stimulation (Figures 1−3). Furthermore pharmacologic blockade of group I mGluRs prevented vascular responses to electrical stimulation in IP$_3$R2$^{+/+}$ slices and had no effect on IP$_3$R2$^{-/-}$ slices (Figure 3C). IP$_3$R2 may also be expressed in cerebrovascular endothelial cells and it is possible that endothelial IP$_3$R2 contributes to the arteriole response to mGluR stimulation [23]. However, it is unlikely that results in the IP$_3$R2$^{-/-}$ slices can be attributed to loss of endothelial IP$_3$R2 because both blockade of mGluRs in IP$_3$R2$^{+/+}$ slices and cPLA$_2\alpha$ deficiency eliminated the responses to electrical stimulation (Figures 3C and 5). The role of endothelial IP$_3$R2 in vascular responses can be explicitly tested using endothelial denuded cerebral arterioles in future studies [24]. These results also demonstrate that the diacylglycerol produced by PLC activation is not sufficient to regulate arteriole responses.

Previous experiments have used non-specific inhibitors of various PLA$_2$s to suggest that astrocyte Ca^{2+} signaling activates PLA$_2$ and that this activity is required for cerebrovascular regulation [8,10]. For example inhibition of PLA$_2$ in intact mice by application of the drug MAFP to the cortical surface eliminated the response to photo-uncaging of Ca^{2+} in astrocytes [25]. However, the particular molecular form(s) of PLA$_2$ needed for cerebrovascular regulation had not previously been determined. cPLA$_2\alpha$ has been identified in astrocytes but other forms of PLA$_2$ are also expressed in astrocytes [26,27]. Our experiments show that the cPLA$_2\alpha$ is the molecular species that is downstream from IP$_3$R2 activation. We also examined the effect of cPLA$_2\alpha$ expression on the astrocyte Ca^{2+} response following 1S,3R-ACPD treatment. The results of the present Ca^{2+} imaging experiments show that cPLA$_2\alpha$ does not alter the IP$_3$-mediated Ca^{2+} response or impact Ca^{2+} homeostasis in the astrocyte following efflux of Ca^{2+} from the endoplasmic reticulum in the astrocyte.

cPLA$_2\alpha$ activity is regulated by phosphorylation and transloca-tion to its membrane substrate. Translocation of cPLA$_2\alpha$ to cellular membranes requires Ca^{2+} binding to the C2 domain of the protein [28] while enzymatic activity is modulated by phosphor-ylation at sites that are not part of the C2 domain [29]. The local cellular Ca^{2+} levels, lipid environment and the phosphorylation state of the protein play a role in determining the specific membrane compartment to which cPLA$_2\alpha$ translocates [30]. When astrocyte Ca^{2+} waves were initiated in brain slices by selective photo-uncaging of astrocyte Ca^{2+}, peaks in endfoot Ca^{2+} preceded those in astrocyte soma [8]. Our results demonstrate that mGluR activation causes Ca^{2+} increases in the soma and the foot processes of astrocytes. Local elevation of endfoot Ca^{2+} makes it possible that cPLA$_2\alpha$ translocates to the cytosolic face of these membranes to hydrolyze arachidonic acid at this site. Localization of cPLA$_2\alpha$ to the astrocyte perivascular endfoot could lead to increases in arachidonic acid concentration at the endfoot where it can be metabolized intracellularly or diffuse transcellularly into the neighboring vascular smooth muscle cell [8]. The membrane site of cPLA$_2\alpha$ activity has the potential to profoundly impact the eicosanoids that are generated from arachidonic acid metabolism.

Our results are consistent with a model in which astrocyte cPLA$_2\alpha$ generates the arachidonic acid that is metabolized within the astrocyte for production of prostaglandins and vasodilatory EETs. Astrocytes express COX-1 which metabolizes arachidonic acid to PGH$_2$ which is the precursor for all prostaglandins [25]. PGs, particularly PGE$_2$, are implicated in the arteriole dilation
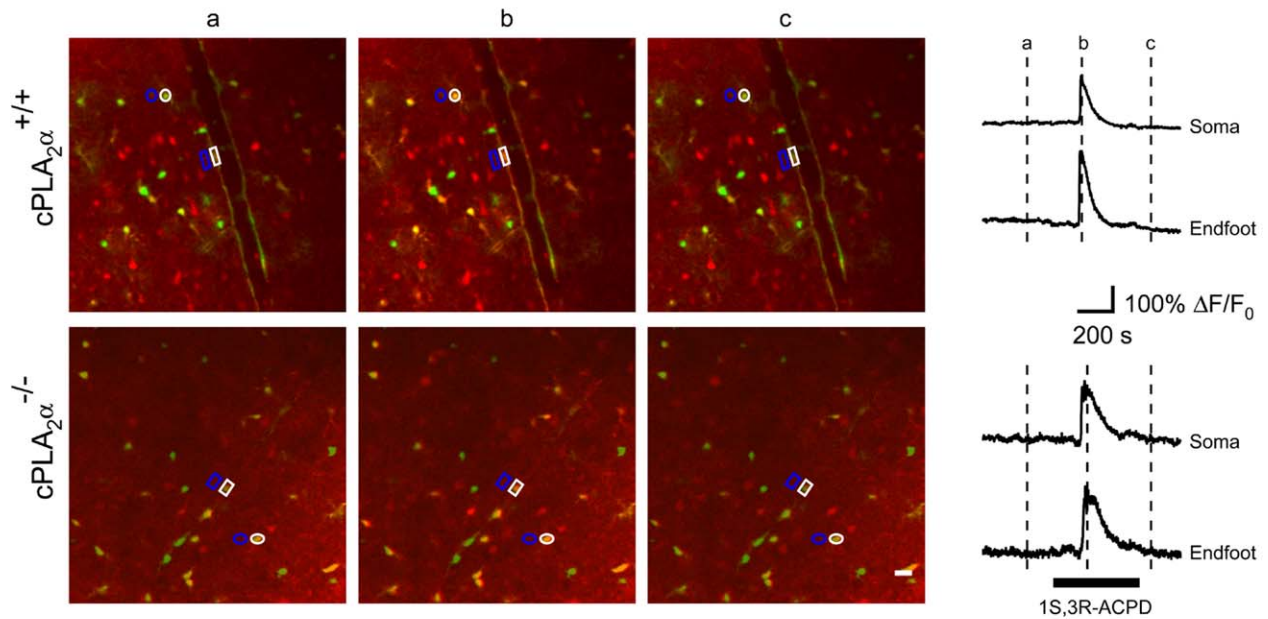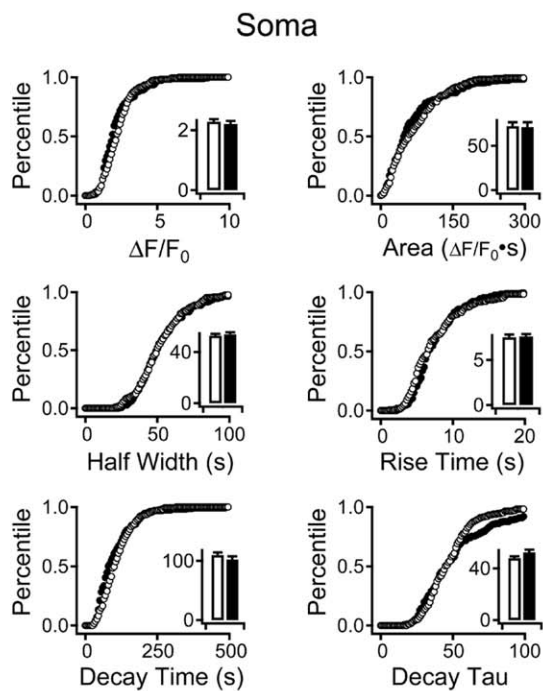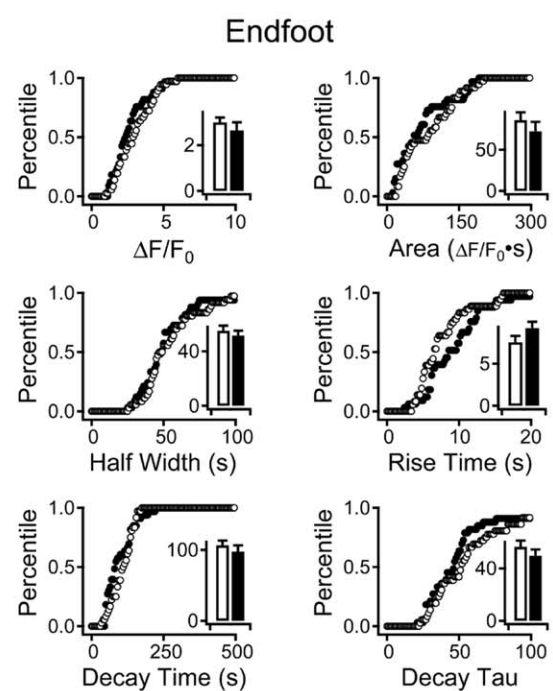
Figure 7. Astrocyte Ca^{2+} responses in neocortical slices to mGluR agonist application are not altered by absence of cPLA$_2\alpha$ expression. Cortical brain slices from S100β-EGFP/cPLA$_2\alpha^{+/+}$ (upper panel) and S100β-EGFP/cPLA$_2\alpha^{-/-}$ (lower panel) mice were loaded with the Ca^{2+}-sensitive fluorophore Rhod-2/AM. Regions of interest representing astrocyte soma (white circles) and vascular foot processes (white box) were identified by EGFP expression and histologic location. Regions of interest representing background fluorescence for soma and endfeet are depicted by blue outlines. Ca^{2+} fluorescence measured for the soma and endfeet are displayed at 3 times in relation to 1S,3R-ACPD treatment: (a) before, (b) at peak response and (c) after. Representative Ca^{2+} measurements for soma and endfeet for each genotype are depicted in the right panel. The time of the 1S, 3R ACPD application is indicated by the black bar. The Ca^{2+} responses of astrocyte populations are shown in **B.** Soma (+/+, n = 169; $^{-/-}$, n = 166) and **C.** endfeet (+/+, n = 36; $^{-/-}$, n = 33) and were measured as Ca^{2+} peak amplitude, area under curve, half width, rise time, decay time or decay tau (as defined in Methods). The graphs show cumulative probability histograms analysis of the astrocyte populations by parameters

response [9]. Cultured cortical astrocytes contain CYP450 epoxygenase activity that metabolizes arachidonic acid to vasodilatory EETs which can regulate cerebral blood flow by transcellular passage from the astrocyte foot process to the VSMC [31,32]. Cerebral vascular smooth muscle cells express CYP450 ω–hydroxylase which metabolizes arachidonic acid to form 20-HETE [33]. The production of 20-HETE inhibits BK channels while increasing open probability of the L-type Ca^{2+} channels of the VSMC, leading to VSMC and arteriole constriction [34]. When cPLA$_2\alpha$ translocates to the vascular foot process arachidonic acid can diffuse into the VSMC where it is metabolized to vasoconstrictive 20-HETE. In agreement with our results on 1S,3R-ACPD-treated, naïve brain slices, a non-specific PLA$_2$ inhibitor prevented the constrictive response following uncaging of Ca^{2+} in mouse cortical brain slices [8]. Also consistent with our findings, treatment of rat brain slices with the combination of the thromboxane receptor agonist U-46619 and the non-specific PLA$_2$ inhibitor methyl arachidonyl fluorophosphanate (MAFP) significantly reduced the arteriole response to 1S,3R-ACPD treatment [10].

If the roles of IP$_3$ and cPLA$_2\alpha$ in cerebrovascular regulation are simply to regulate the release of arachidonic acid in astrocytes for metabolism into both eicosanoid vasodilators and vasoconstrictors, what determines the response of the vessel? Our results provide some new insight into this process.

The initial diameter of an arteriole is determined by the balance between signals for constriction and dilation on the VSMC. Previous studies conducted in 95% O$_2$ with rat brain slices suggested that the initial arteriole diameter determines the directionality and magnitude of changes in diameter following stimulation [10]. Arterioles in naïve slices are not pressurized and therefore lack intrinsic tone and are relatively dilated. Therefore, an arteriole in a naïve slice may be more responsive to constrictive stimuli [8,35]. In contrast, pretreatment with U-46619 causes vasoconstriction that favors dilation following activation of the astrocyte [10]. As we observed, absence of the IP$_3$R2-cPLA$_2\alpha$ pathway abolishes the vasomotor effects of mGluR activation regardless of the resting diameter of the arteriole. This indicates that this signaling pathway is required for elaboration of both vasoconstrictors and dilators.

The balance of the metabolism of arachidonic acid between CYP450 and cyclooxygenase enzymes appears to be essential for neurovascular regulation [36,37]. Post-synaptic neurons also release NO and NO has been implicated in determining the metabolic balance between synthesis of EETs and 20-HETE [11]. We electrically stimulated slices in order to evaluate the effect of neuron activation on the cPLA$_2\alpha$ and IP$_3$R2-dependent vascular regulatory pathways. Electrical stimulation resulted in astrocyte Ca^{2+} responses (Supporting Figure S2) and does not directly activate VSMC [38]. In our study, electrical stimulation caused dilation in both the naïve and U-46619 preconstricted arterioles while it had no vasomotor effect on IP$_3$R2$^{-/-}$ or cPLA$_2\alpha^{-/-}$ arterioles. This implies that electrical activation of neurons (as compared to 1S,3R-ACPD activation of astrocytes) either increases the relative amount of a cPLA$_2\alpha$-dependent vasodilator or decreases the amount a of cPLA$_2\alpha$-dependent vasoconstrictor that is produced by activation of the astrocyte IP$_3$R2. A mechanism for neuronal regulation of the astrocyte cPLA$_2\alpha$-dependent response was first suggested by the finding that NO inhibits the synthesis of EETS and 20-HETE [39]. Indeed, in rat

retinas NO appears to be a determinant in the polarity of light-induced vascular responses with NO production favoring vasoconstriction because epoxygenanse activity (metabolizes arachidonic acid to EET, a vasodilator) is inhibited at lower NO concentrations than is Ω-hydroxylase (metabolizes arachidonic acid to 20-HETE, a vasoconstrictor) [11]. We found that inhibition of neuronal NOS with L-NPA pre-treatment prevented the electrical stimulation-induced dilation in cPLA$_2\alpha^{+/+}$ slices. We hypothesize that electrical stimulation causes neuronal NO release which inhibits production of 20-HETE in the VSMC [40]. In contrast, when nNOS is inhibited by L-NPA the Ω-hydroxylase is no longer blocked by NO and production of 20-HETE causes arteriole constriction that opposes the dilating effects of EETs and PGs. In agreement with our results Liu et al. (2008) tested the effect of NOS expression on functional hyperemia in the whisker barrel cortex of rats and concluded that increased NO production following whisker stimulation may suppress 20-HETE synthesis [21]. Taken together, our data indicate that the vascular response to astrocyte Ca^{2+} signaling depends upon both the pre-existing tone of the arteriole and the particular signaling pathways that a stimulus triggers.

Our experiments also demonstrate that regulation of cerebral arteriole responses to vasoactive eicosanoids is dependent upon levels of tissue oxygenation. We used PGE$_2$ to demonstrate that arteriole responses remained intact at the conclusion of each series of measurements. As expected, the response to PGE$_2$ was independent of the IP$_3$R2 or cPLA$_2\alpha$ expression in the slice because PGE$_2$ is a downstream metabolite of arachidonic acid. To our surprise, 10 μM PGE$_2$ bath application caused arteriole constriction in the 95% O$_2$ and dilation in the 20% O$_2$ environment. This result is identical to the responses seen with activation of the mGluR and is consistent with a model in which the response to PGE$_2$ is dependent on the metabolic and oxidative state of the region. In other studies, in rat brain slices, similar doses of PGE$_2$ were described as an arteriole vasodilator [5,9]. In one of these studies the slices were maintained in an ACSF solution with 2.8 mM glucose in contrast to the 20 mM glucose used in our ACSF [5]. This lower glucose concentration could favor glycolysis and thus dilation [9]. In the other study the response to PGE$_2$ in high O$_2$ was not evaluated while the low O$_2$ response was identical to our result [9]. Because arteriole responses to PGE$_2$ are largely determined by activation of the eicosanoid receptors of the VSMC and vascular endothelial cells we hypothesize that the regional metabolic state could alter the binding of PGE$_2$ on eicosanoid receptors [41]. For example, in renal interlobular arterioles PGE$_2$ causes constriction by binding the prostaglandin E type 3 (EP3) receptor [42] and in rat aortic rings concentrations of PGE$_2$>1 μM cause constriction through activation of the thromboxane A$_2$ receptor [43,44]. We tested the possibility that constriction in 95% O$_2$ was related to the high concentration of PGE$_2$ used in the experiment by performing a dose response titration. In the high O$_2$ environment 100 nM PGE$_2$ still caused arteriole constriction and dilation was not observed at any concentration (not shown). Thus it is possible that the vascular responses to PGE$_2$ are regulated by metabolic state in which high O$_2$ favors binding to prostaglandin E receptors (EP) that cause constriction (EP1 and EP3) relative to those that cause dilation (EP2 and EP4). This hypothesis requires further testing because expression of thromboxane and EP receptors in the brain microvasculature has not been characterized and the dependence

on oxidative state of specific prostaglandin binding on receptors has not been explored [45].

Our work is largely consistent with previous findings using pharmacological inhibition of PLA$_2$s and arachidonic acid metabolic enzymes. This is in contrast to a study in which a cPLA$_2\alpha$-deficient mouse had a normal in vivo circulatory response to sensory stimulation [46]. It has been proposed that in this in vivo study the compensatory mechanisms may overcome the permanent genetic loss of cPLA$_2\alpha$ and maintain normal circulatory responses [38]. Our work demonstrates that this is not the case since there is no evidence of compensation in the vascular responses of our knock-out mice in the slice preparation. It is also important to note that the kinetics of the vascular response in the slice model are significantly slower than those measured in vivo. Our results are consistent with previously published work using similar slice conditions. For example, Gordon and colleagues found that in high O$_2$ concentration constriction was maximal 4 minutes after stimulation while dilation peaked 17 minutes after stimulation [9]. The slow kinetics of the slice model may be due to a number of factors. Vessel diameters are determined by the summation of constrictive and relaxing forces and the rates of change in diameter are likely due to the size of gradients in these forces. The lack of arteriole pressure in brain slice arterioles will decrease the dilation gradient and it is possible that contractile pressures are also reduced as the tissue of a slice can easily expand. Our results are also consistent with a pathway in which multiple sequential enzymatic steps are required to generate vasoactive compounds. It is possible that bath perfusion of the slices delays achieving the maximum concentration of arachidonic acid metabolites. Another possible reason for the difference between the in vivo and in slice models is the normal pH that we used to maintain slice health. The metabolic state of astrocytes impacts the polarity of vascular responses and regional acidosis appears to have a profound impact [9]. cPLA$_2\alpha$ activity is sensitive to pH and it is possible that metabolic alterations that lower cellular pH could decrease cPLA$_2\alpha$ activity within the astrocyte. Finally, it is likely that other regulatory pathways exist in vivo but not in slice. There are likely to be many other factors that influence cerebral vascular regulation.

The magnitude of the stimulated astrocyte Ca^{2+} response may also determine whether an arteriole constricts or dilates [38]. We found that the presence or absence of cPLA$_2\alpha$ had no apparent effect on the Ca^{2+} response of astrocytes to 1S,3R-ACPD (Figure 7). Similarly the treatment of the slices with U-46619 did not cause any immediate Ca^{2+} response in the astrocytes nor did it alter the relative Ca^{2+} response of astrocytes in slices that were subsequently treated with 1S,3R-ACPD (not shown). This is consistent with an absence of thromboxane A$_2$ receptors in perivascular astrocytes [47]. Indeed while addition of U-46619 alters the resting tone and Ca^{2+} responsiveness of the vascular smooth muscle cells of the arterioles [48] it appears to have little, if any effect upon the perivascular astrocytes. Therefore the changes in polarity of the arteriole response to 1S,3R-ACPD are unlikely to be due to changes in the concentration of Ca^{2+} within the astrocyte. In this model, astrocyte cPLA$_2\alpha$ generates arachidonic acid and the responses of the vascular system to this arachidonic acid release are determined by its metabolism and other factors.

While other investigations have used bath application of U-46619 to achieve an equilibrium arteriole diameter in brain slices [10] we were not able to replicate this result. Bath application with 100 nM U-46619 caused progressive arteriole constriction that did not equilibrate. In preliminary work we found that higher concentrations of U-46619 caused arteriole occlusion and prevented subsequent responses to chemical dilators and constric-

tors. Application of lower concentrations of U-46619 slowed the constrictive response but did not achieve a stable arteriole diameter within the time frame of the experiments (not shown). In a model that continuously bath applies a dose of U-46619 that is ~5 fold above the EC$_{50}$ for thromboxane receptor occupancy it is not surprising that constriction progresses until the arteriole is completely constricted [49].

Neurons, smooth muscle, and endothelial cells also express cPLA$_2\alpha$ [50–52] and because cPLA$_2\alpha$ is globally deficient in the cPLA$_2\alpha^{-/-}$ mouse we must qualify our conclusions. While the results of this study are consistent with the model in which astrocyte cPLA$_2\alpha$ is the generator of arachidonic acid mediators it remains possible that other cellular sources of cPLA$_2\alpha$ are important in this signaling process. It will be necessary to create cell-line specific gene deletions to further test these possibilities.

We recognize that these experiments leave questions that can be answered by future investigations both in brain slices and in vivo. Our results indicate that activation of the mGluR triggers Ca^{2+} release through the IP$_3$R2 receptor and that this increased Ca^{2+} allows cPLA$_2\alpha$ to release arachidonic acid which is metabolized to vasoactive metabolites. Other forms of PLA$_2$ can act synergistically with cPLA$_2\alpha$ to amplify arachidonic acid release and lipid mediator generation [53] so while cPLA$_2\alpha$ may be the first PLA$_2$ activity in the signaling pathway others may also be necessary. Synaptic activity and the resting tone of the VSMC influence the magnitude and direction of arteriole responses to stimulation and their precise interactions with cPLA$_2$ require further investigation. Importantly while cPLA$_2\alpha$ blockade appears to be neuroprotective in excitotoxicity models the current results suggest that chemical inhibition of cPLA$_2\alpha$ may significantly impair normal mechanisms of neurovascular regulation [54,55].

Methods

Slice Preparation and Imaging

Brains were removed from P20–35 mice after decapitation. Coronal slices of the somatosensory cortex (300 µm thick) were cut on a Leica VT1200S vibrating tissue slicer (Leica Biosystems, Richmond, IL) equipped with a sapphire blade in ice-cold cutting saline (in mM): 135 N-methyl-D-glucamine chloride (NMDG), 1 KCl, 1.2 KH$_2$PO$_4$, 0.5 CaCl$_2$, 1.5 MgCl$_2$, 24.2 Choline Bicarbonate, 13 glucose, adjusted to pH 7.4 and oxygenated with 95% O$_2$/5% CO$_2$. Slices were then maintained in ACSF (in mM): 125 NaCl, 2.5 KCl, 1 NaH$_2$PO$_4$, 26.2 NaHCO$_3$, 2.5 CaCl$_2$, 1.3 MgCl$_2$, 20 glucose (pH = 7.4), for at least 1 h at room temperature. For recording and imaging, slices were placed in a submerged chamber superfused with ACSF at a rate of 1–2 ml/ min at 34°C. A 10 minute period of baseline recording preceded brain slice stimulation. For experiments with 1S,3R-ACPD, this drug was bath applied at indicated concentrations for 10 min followed by a 10 min washout period. Following this, the responsiveness of the chosen arteriole was evaluated by the addition of PGE$_2$. In experiments with U-46619 was added to the ACSF after the initial 10 min stabilization period at the indicated concentrations and applied continuously throughout the experiments. For electrical stimulation, a concentric bipolar electrode was placed 200–300 µm lateral to the arteriole of interest. The stimulation protocol consisted of 100 Hz monophasic pulse trains of duration 200 msec, with an intertrain interval of 5 sec for a total duration of 4 min.

Cell structure within cortical slices was visualized through a 40X water immersion objective with gradient contrast optics using a fixed-stage upright microscope equipped with a Zeiss Pascal confocal system with Argon ion (488 nm), and HeNe (543 nm)

lasers. Arterioles in each slice were identified by their characteristic size (inner diameter of 5–20 µm) and the presence of a vascular smooth muscle layer. We selected arterioles from cortical layers 2–5 that could be observed for a minimum length of 200 µm and then measured changes in the inner diameter. For each arteriole a baseline image was obtained and we established between 5–10 reference lines across the arteriole lumen. These reference lines were spaced at ∼5 µm intervals and were applied at the same axial location of the vessel for all subsequent radial measurements. At each time point one arteriole image was obtained and a second was obtained 30 seconds later. These images were digitally superimposed and radial measurements were taken from the resultant image. An investigator who was blinded to the experimental condition and genotype of the slice measured the arteriolar internal diameter for each time point.

After cutting, slices were incubated in ACSF saturated with 95% O$_2$/5% CO$_2$ for 60 minutes. They were transferred and maintained in ACSF saturated with either 95% O$_2$/5% CO$_2$ or 20% O$_2$/5% CO$_2$ depending upon the experiment. For low O$_2$ experiments, slices were equilibrated in 20% O$_2$ saturated ACSF for at least 40 min before experiments. The switch from high O$_2$ to low O$_2$ caused a small constriction of vessels (1.50±0.84%, P = 0.095, n = 17).

To block group I mGluRs, 100 nM JNJ (an antagonist of mGlu$_1$) and 10 µM MPEP (an antagonist of mGlu$_5$) were bath applied for 30 min before electrical stimulation. Blockade of mGluRs did not change vessel tone (dilation: 0.86±1.83%, P = 0.65, n = 9). JNJ and MPEP were dissolved in ethanol (final ethanol concentration: 0.02%).

To eliminate NO generated by neurons 10 µM L-NPA, a highly selective nNOS inhibitor, was bath applied for 60 min before electrical stimulation. L-NPA had little effect on vessel tone (constriction:1.46±1.93%, P = 0.47, n = 9). L-NPA was dissolved in water.

We used Rhod-2/AM as a cell-permeant indicator for Ca^{2+} imaging experiments. It was dissolved in DMSO together with the detergent Pluronic F-127 and then diluted with HEPES-ACSF (in mM) (125 NaCl, 2.5 KCl, 1 NaH$_2$PO$_4$, 25 HEPES, 2.5 CaCl$_2$, 1.3 MgCl$_2$, 20 glucose, adjusted pH to 7.4) to a final concentration of 10 µM (final DMSO concentration: 0.23%). Because the Ca^{2+} indicator Rhod-2/AM preferentially loads astrocytes [8] slices were incubated with Rhod-2/AM for 60–90 min at room temperature. Following loading, slices were maintained in ACSF. Astrocytes were selected for imaging on the basis of their uptake of Rhod-2 (or expression of EGFP), an ameboid-shaped cell body, a location in direct proximity to an arteriole, and the presence of a foot process in proximity to the arteriole. Rhod-2 was excited with 543 nm light while EGFP, marking a subpopulation of astrocytes of S100β-EGFP transgenic mice, was excited with 488 nm light. In this preparation 82±3% of EGFP astrocytes were loaded with red Rhod-2/AM (335 of cells, 17 slices, 8 mice). Rhod-2 images were acquired at 1.3 Hz/frame and signals were expressed as ΔF/F$_0$ = (F$_t$-F$_0$)/(F$_0$-B$_0$), where F$_t$ is fluorescence intensity at any given time, F$_0$ is the average fluorescence intensity in the baseline period and B$_0$ is the average fluorescence intensity of background. Background values were taken from an adjacent region of interest (see Figure 7). For analysis of Ca^{2+} transients the 10–90% rise time and 90–10% decay times were calculated. Group data were expressed as mean ± SEM and compared by Student's t-test.

Mice

Mice were housed with a 12-hour diurnal light cycle and free access to food and water. All genetically altered mice used for experiments were produced by mating male and female mice that were heterozygous for the gene of interest. In these studies we used cPLA$_2\alpha^{+/+}$ and cPLA$_2\alpha^{-/-}$ mice [54] that had been backcrossed on the BALB/C strain for >10 generations. Mice that were previously engineered to express a transgene for the EGFP protein under the control of the S100β promoter [22] were bred for greater than 6 generations with F1 progeny of BALB/c x cPLA$_2\alpha^{-/-}$ mating to create S100β-eGFP-cPLA$_2\alpha^{+/-}$ mice. IP$_3$R2$^{-/-}$ mice were originally supplied on the Swiss Webster background (Ju Chen, personal communication) and were mated with BALB/c WT mice to generate IP$_3$R2$^{+/-}$ mice [56]. All genotyping was performed from tail samples on mice between the ages of 8–12 days and were analyzed by PCR using specific primer pairs.

Ethics

All studies were conducted with the approval of the Johns Hopkins University Animal Care and Use Committee under the protocol numbers MO07M135 and MO10M69. Performance of the studies was also in accordance with the guidelines of the National Institutes of Health and the National Research Council.

Data Analysis

Changes in Rhod-2 fluorescence were analyzed using IGOR Pro 6 (Wavemetrics, Inc. Portland, OR) and expressed as cumulative probability histograms and mean values ± S.E.M. Arteriole diameters were measures using NIH Image J (NIH, Bethesda, MD) and expressed as mean values ± S.E.M. Data between groups were compared by Student's t-test.

Reagents

1,1,1-trifluoro-6Z,9Z,12Z,15Z-heneicosatetraen-2-one (arachidonyl trifluoromethyl ketone, ATK), supplied as a solution in ethanol; final ethanol concentration: 0.0375%), PGE$_2$ (supplied as a crystalline solid, dissolved in ethanol, final ethanol concentration: 0.35%), and U-46619 (supplied as a solution in methyl acetate, final methyl acetate concentration: 0.0007%) were purchased from Cayman Chemical Co. (Ann Arbor, MI). (1S,3R)-1-Aminocyclopentane-1,3-dicarboxylic acid (1S,3R-ACPD), Nω-propyl-l-arginine (L-NPA), JNJ 16259685, and 2-Methyl-6-(phenylethynyl)pyridine hydrochloride (MPEP) *were purchased from Tocris bioscience* (Ellisville, MO), and Rhod-2/AM was purchased from Invitrogen Corp. (Carlsbad, CA). All other chemicals were purchased from Sigma (St. Louis, MO). cPLA$_2\alpha$ heterozygous mice bred into the BALB/C strain were used for all matings and were the gift of Joseph V. Bonventre (Brigham and Women's Hospital, Boston, MA) [54]. IP$_3$ type-2 receptor-deficient mice (IP$_3$R2$^{-/-}$) were the gift of Ju Chen (University of California, San Diego, CA) [56]. Mice expressing the EGFP protein under the control of the S100β promoter were originally created in the laboratory of Legraverend (Institut de Génomique Fonctionnelle, Montpellier, France) [22] and were provided by Dwight E. Bergles (Johns Hopkins University, Baltimore, MD).

Supporting Information

Figure S1 Change in diameter of cortical arterioles upon sequential, combined exposure to U46619 and PGE$_2$. Cortical brain slices from IP$_3$R2$^{+/+}$ mice were at equilibrium with 95% O$_2$, and treated with 100 nM U-46619 supplemented ACSF for 30 min. After 30 min ACSF was further supplemented with 10 µM PGE$_2$ for an additional 10 min. n = 9 arterioles.
(TIF)

Figure S2   Change in diameter of a single arteriole upon sequential, combined exposure to U46619 and 1S, 3R-ACPD. Time is expressed in minutes with the $t = 0$ set at the initiation of U46619 and the initial diameter at $t = -10$ minutes. Bars indicate the time of bath application of 100 nM U46619 or 50 µM 1S, 3R-ACPD.
(TIF)

Figure S3   Electrical stimulation evokes Ca^{2+} transient in astrocytes of a cortical slice derived from an S100β-EGFP mouse. Slices were loaded with Rhod-2/AM and a concentric bipolar electrode was placed 200–300 µm from the region of interest. Rhod-2 fluorescence (red) in multiple astrocyte cell bodies that express EGFP (green) (circled in white; left panel) was measured after stimulation at 100 Hz for 200 ms (expanded

black bar, right panel). The Ca^{2+} fluorescence signals of individual astrocytes are plotted. Scale bar: 20 µM.
(TIF)

Acknowledgments

Author Contributions

Conceived and designed the experiments: LH DJL AS. Performed the experiments: LH. Analyzed the data: LH. Contributed reagents/materials/analysis tools: DJL AS. Wrote the paper: LH DJL AS.

References

1. Attwell D, Buchan AM, Charpak S, Lauritzen M, Macvicar BA, et al. (2010) Glial and neuronal control of brain blood flow. Nature 468: 232–243.
2. Koehler RC, Roman RJ, Harder DR (2009) Astrocytes and the regulation of cerebral blood flow. Trends Neurosci 32: 160–169.
3. Oberheim NA, Takano T, Han X, He W, Lin JH, et al. (2009) Uniquely hominid features of adult human astrocytes. J Neurosci 29: 3276–3287.
4. Simard M, Nedergaard M (2004) The neurobiology of glia in the context of water and ion homeostasis. Neuroscience 129: 877–896.
5. Zonta M, Angulo MC, Gobbo S, Rosengarten B, Hossmann KA, et al. (2003) Neuron-to-astrocyte signaling is central to the dynamic control of brain microcirculation. Nat Neurosci 6: 43–50.
6. Foskett JK, White C, Cheung KH, Mak DO (2007) Inositol trisphosphate receptor Ca^{2+} release channels. Physiol Rev 87: 593–658.
7. Balboa MA, Varela-Nieto I, Killermann Lucas K, Dennis EA (2002) Expression and function of phospholipase A$_2$ in brain. FEBS Lett 531: 12–17.
8. Mulligan SJ, MacVicar BA (2004) Calcium transients in astrocyte endfeet cause cerebrovascular constrictions. Nature 431: 195–199.
9. Gordon GR, Choi HB, Rungta RL, Ellis-Davies GC, MacVicar BA (2008) Brain metabolism dictates the polarity of astrocyte control over arterioles. Nature 456: 745–749.
10. Blanco VM, Stern JE, Filosa JA (2008) Tone-dependent vascular responses to astrocyte-derived signals. Am J Physiol Heart Circ Physiol 294: H2855–2863.
11. Metea MR, Newman EA (2006) Glial cells dilate and constrict blood vessels: a mechanism of neurovascular coupling. J Neurosci 26: 2862–2870.
12. Clark JD, Lin LL, Kriz RW, Ramesha CS, Sultzman LA, et al. (1991) A novel arachidonic acid-selective cytosolic PLA$_2$ contains a Ca^{2+}-dependent translocation domain with homology to PKC and GAP. Cell 65: 1043–1051.
13. Leis HJ, Windischhofer W (2008) Inhibition of cyclooxygenases 1 and 2 by the phospholipase-blocker, arachidonyl trifluoromethyl ketone. Br J Pharmacol 155: 731–737.
14. Song H, Ramanadham S, Bao S, Hsu FF, Turk J (2006) A bromoenol lactone suicide substrate inactivates group VIA phospholipase A$_2$ by generating a diffusible bromomethyl keto acid that alkylates cysteine thiols. Biochemistry 45: 1061–1073.
15. Petravicz J, Fiacco TA, McCarthy KD (2008) Loss of IP$_3$ receptor-dependent Ca^{2+} increases in hippocampal astrocytes does not affect baseline CA1 pyramidal neuron synaptic activity. J Neurosci 28: 4967–4973.
16. Sharp AH, Nucifora FC, Blondel O, Sheppard CA, Zhang C, et al. (1999) Differential cellular expression of isoforms of inositol 1,4,5-triphosphate receptors in neurons and glia in brain. J Comp Neurol 406: 207–220.
17. Norel X (2007) Prostanoid receptors in the human vascular wall. ScientificWorldJournal 7: 1359–1374.
18. Abramovitz M, Adam M, Boie Y, Carriere M, Denis D, et al. (2000) The utilization of recombinant prostanoid receptors to determine the affinities and selectivities of prostaglandins and related analogs. Biochim Biophys Acta 1483: 285–293.
19. Bingham CO, 3rd, Austen KF (1999) Phospholipase A$_2$ enzymes in eicosanoid generation. Proc Assoc Am Physicians 111: 516–524.
20. Ma J, Ayata C, Huang PL, Fishman MC, Moskowitz MA (1996) Regional cerebral blood flow response to vibrissal stimulation in mice lacking type I NOS gene expression. Am J Physiol 270: H1085–1090.
21. Liu X, Li C, Falck JR, Roman RJ, Harder DR, et al. (2008) Interaction of nitric oxide, 20-HETE, and EETs during functional hyperemia in whisker barrel cortex. Am J Physiol Heart Circ Physiol 295: H619–631.
22. Vives V, Alonso G, Solal AC, Joubert D, Legraverend C (2003) Visualization of S100β-positive neurons and glia in the central nervous system of EGFP transgenic mice. J Comp Neurol 457: 404–419.
23. Hertle DN, Yeckel MF (2007) Distribution of inositol-1,4,5-trisphosphate receptor isotypes and ryanodine receptor isotypes during maturation of the rat hippocampus. Neuroscience 150: 625–638.
24. Barkoudah E, Jaggar JH, Leffler CW (2004) The permissive role of endothelial NO in CO-induced cerebrovascular dilation. Am J Physiol Heart Circ Physiol 287: H1459–1465.
25. Takano T, Tian GF, Peng W, Lou N, Libionka W, et al. (2006) Astrocyte-mediated control of cerebral blood flow. Nat Neurosci 9: 260–267.
26. Lautens LL, Chiou XG, Sharp JD, Young WS, 3rd, Sprague DL, et al. (1998) Cytosolic phospholipase A$_2$ (cPLA$_2$) distribution in murine brain and functional studies indicate that cPLA$_2$ does not participate in muscarinic receptor-mediated signaling in neurons. Brain Res 809: 18–30.
27. Xu J, Chalimoniuk M, Shu Y, Simonyi A, Sun AY, et al. (2003) Prostaglandin E$_2$ production in astrocytes: regulation by cytokines, extracellular ATP, and oxidative agents. Prostaglandins Leukot Essent Fatty Acids 69: 437–448.
28. Nalefski EA, McDonagh T, Somers W, Seehra J, Falke JJ, et al. (1998) Independent folding and ligand specificity of the C2 calcium-dependent lipid binding domain of cytosolic phospholipase A$_2$. J Biol Chem 273: 1365–1372.
29. Tucker DE, Ghosh M, Ghomashchi F, Loper R, Suram S, et al. (2009) Role of phosphorylation and basic residues in the catalytic domain of cytosolic phospholipase A$_2$ alpha in regulating interfacial kinetics and binding and cellular function. J Biol Chem 284: 9596–9611.
30. Leslie CC, Gangelhoff TA, Gelb MH (2010) Localization and function of cytosolic phospholipase A$_2$ alpha at the Golgi. Biochimie 92: 620–626.
31. Alkayed NJ, Birks EK, Hudetz AG, Roman RJ, Henderson L, et al. (1996) Inhibition of brain P-450 arachidonic acid epoxygenase decreases baseline cerebral blood flow. Am J Physiol 271: H1541–1546.
32. Alkayed NJ, Narayanan J, Gebremedhin D, Medhora M, Roman RJ, et al. (1996) Molecular characterization of an arachidonic acid epoxygenase in rat brain astrocytes. Stroke 27: 971–979.
33. Harder DR, Roman RJ, Gebremedhin D (2000) Molecular mechanisms controlling nutritive blood flow: role of cytochrome P450 enzymes. Acta Physiol Scand 168: 543–549.
34. Gebremedhin D, Lange AR, Lowry TF, Taheri MR, Birks EK, et al. (2000) Production of 20-HETE and its role in autoregulation of cerebral blood flow. Circ Res 87: 60–65.
35. Fergus A, Jin Y, Thai QA, Kassell NF, Lee KS (1995) Vasodilatory actions of calcitonin gene-related peptide and nitric oxide in parenchymal microvessels of the rat hippocampus. Brain Res 694: 78–84.
36. Gordon GR, Mulligan SJ, MacVicar BA (2007) Astrocyte control of the cerebrovasculature. Glia 55: 1214–1221.
37. Harder DR, Alkayed NJ, Lange AR, Gebremedhin D, Roman RJ (1998) Functional hyperemia in the brain: hypothesis for astrocyte-derived vasodilator metabolites. Stroke 29: 229–234.
38. Girouard H, Bonev AD, Hannah RM, Meredith A, Aldrich RW, et al. (2010) Astrocytic endfoot Ca^{2+} and BK channels determine both arteriolar dilation and constriction. Proc Natl Acad Sci USA 107: 3811–3816.
39. Alonso-Galicia M, Drummond HA, Reddy KK, Falck JR, Roman RJ (1997) Inhibition of 20-HETE production contributes to the vascular responses to nitric oxide. Hypertension 29: 320–325.
40. Alonso-Galicia M, Hudetz AG, Shen H, Harder DR, Roman RJ (1999) Contribution of 20-HETE to vasodilator actions of nitric oxide in the cerebral microcirculation. Stroke 30: 2727–2734; discussion 2734.
41. Feletou M, Huang Y, Vanhoutte PM (2010) Vasoconstrictor prostanoids. Pflugers Arch 459: 941–950.
42. van Rodijnen WF, Korstjens IJ, Legerstee N, Ter Wee PM, Tangelder GJ (2007) Direct vasoconstrictor effect of prostaglandin E$_2$ on renal interlobular arteries: role of the EP3 receptor. Am J Physiol Renal Physiol 292: F1094–1101.
43. Dorn GW, 2nd, Becker MW, Davis MG (1992) Dissociation of the contractile and hypertrophic effects of vasoconstrictor prostanoids in vascular smooth muscle. J Biol Chem 267: 24897–24905.
44. Tang EH, Jensen BL, Skott O, Leung GP, Feletou M, et al. (2008) The role of prostaglandin E and thromboxane-prostanoid receptors in the response to prostaglandin E$_2$ in the aorta of Wistar Kyoto rats and spontaneously hypertensive rats. Cardiovasc Res 78: 130–138.

45. Sugimoto Y, Narumiya S, Ichikawa A (2000) Distribution and function of prostanoid receptors: studies from knockout mice. Prog Lipid Res 39: 289–314.

46. Kitaura H, Uozumi N, Tohmi M, Yamazaki M, Sakimura K, et al. (2007) Roles of nitric oxide as a vasodilator in neurovascular coupling of mouse somatosensory cortex. Neurosci Res 59: 160–171.

47. Borg C, Lim CT, Yeomans DC, Dieter JP, Komiotis D, et al. (1994) Purification of rat brain, rabbit aorta, and human platelet thromboxane A$_2$/prostaglandin H$_2$ receptors by immunoaffinity chromatography employing anti-peptide and anti-receptor antibodies. J Biol Chem 269: 6109–6116.

48. Neppl RL, Lubomirov LT, Momotani K, Pfitzer G, Eto M, et al. (2009) Thromboxane A$_2$-induced bi-directional regulation of cerebral arterial tone. J Biol Chem 284: 6348–6360.

49. Schnackenberg CG, Welch WJ, Wilcox CS (2000) TP receptor-mediated vasoconstriction in microperfused afferent arterioles: roles of O$_2^-$ and NO. Am J Physiol Renal Physiol 279: F302–308.

50. Kishimoto K, Li RC, Zhang J, Klaus JA, Kibler KK, et al. (2010) Cytosolic phospholipase A$_2$ alpha amplifies early cyclooxygenase-2 expression, oxidative stress and MAP kinase phosphorylation after cerebral ischemia in mice. J Neuroinflammation 7: 42.

51. Mashimo M, Hirabayashi T, Murayama T, Shimizu T (2008) Cytosolic PLA$_2$ alpha activation in Purkinje neurons and its role in AMPA-receptor trafficking. J Cell Sci 121: 3015–3024.

52. Shibata N, Kakita A, Takahashi H, Ihara Y, Nobukuni K, et al. Increased expression and activation of cytosolic phospholipase A$_2$ in the spinal cord of patients with sporadic amyotrophic lateral sclerosis. Acta Neuropathol 119: 345–354.

53. Han WK, Sapirstein A, Hung CC, Alessandrini A, Bonventre JV (2003) Cross-talk between cytosolic phospholipase A$_2$ alpha (cPLA$_2$ alpha) and secretory phospholipase A$_2$ (sPLA$_2$) in hydrogen peroxide-induced arachidonic acid release in murine mesangial cells: sPLA$_2$ regulates cPLA$_2$ alpha activity that is responsible for arachidonic acid release. J Biol Chem 278: 24153–24163.

54. Bonventre JV, Huang Z, Taheri MR, O'Leary E, Li E, et al. (1997) Reduced fertility and postischaemic brain injury in mice deficient in cytosolic phospholipase A$_2$. Nature 390: 622–625.

55. Shen Y, Kishimoto K, Linden DJ, Sapirstein A (2007) Cytosolic phospholipase A$_2$ alpha mediates electrophysiologic responses of hippocampal pyramidal neurons to neurotoxic NMDA treatment. Proc Natl Acad Sci USA 104: 6078–6083.

56. Li X, Zima AV, Sheikh F, Blatter LA, Chen J (2005) Endothelin-1-induced arrhythmogenic Ca^{2+} signaling is abolished in atrial myocytes of inositol-1,4,5-trisphosphate(IP$_3$)-receptor type 2-deficient mice. Circ Res 96: 1274–1281.